Vaccine 37 (2019) 7155–7164

Contents lists available at ScienceDirect

Vaccine

journal homepage: www.elsevier.com/locate/vaccine

Genotypic and phenotypic characterization of West Nile virus NS5 methyltransferase mutants

Jaclyn A. Kaiser [a], Huanle Luo [a], Steven G. Widen [b], Thomas G. Wood [b], Claire Y.-H. Huang [e], Tian Wang [a,c,d], Alan D.T. Barrett [a,c,d,*]

[a] Department of Microbiology and Immunology, University of Texas Medical Branch, Galveston, TX 77555, United States
[b] Molecular Genomics Core Facility, University of Texas Medical Branch, Galveston, TX 77555, United States
[c] Department of Pathology, University of Texas Medical Branch, Galveston, TX 77555, United States
[d] Sealy Institute for Vaccine Sciences, University of Texas Medical Branch, Galveston, TX 77555, United States
[e] Division of Vector-Borne Diseases, Centers for Disease Control and Prevention, Fort Collins, CO 80521, United States

ARTICLE INFO

Article history:
Received 28 May 2019
Received in revised form 5 September 2019
Accepted 11 September 2019
Available online 11 October 2019

Keywords:
Flavivirus
West Nile virus
Attenuation
Methyltransferase
NS5 protein

ABSTRACT

Although West Nile virus (WNV) causes annual cases of neurological disease and deaths in humans, a vaccine has not been licensed for human use. Several WNV genes have been targeted for mutagenesis in attempts to generate live attenuated vaccine candidates, including the non-structural protein NS5. Specifically, mutation of WNV NS5-K61A or NS5-E218A in the catalytic tetrad of the methyltransferase decreases enzyme activity of the NS5 protein and correspondingly attenuates the virus in mice. In this report, NS5-K61A, NS5-E218A, and a double mutant encoding both mutations (NS5-K61A/E218A) were compared both *in vitro* and *in vivo*. Each single mutant was strongly attenuated in highly susceptible outbred mice, whereas the double mutant unexpectedly was not attenuated. Sequencing analysis demonstrated that the double mutant was capable of reversion at both residues NS5-61 and NS5-218, whereas the genotype of the single mutants did not show evidence of reversion. Overall, either NS5-K61A or NS5-E218A methyltransferase mutations could be potential mutations to include in a candidate live WNV vaccine; however, multiple mutations in the catalytic tetrad of the methyltransferase are not tolerated.

1. Introduction

West Nile virus (WNV), a mosquito-borne flavivirus, is responsible for annual outbreaks of neurological disease in the United States (US) [1]. Specifically, from 2002 to 2018 the US Centers for Disease Control and Prevention reported between 386 and 2946 annual cases of West Nile neuroinvasive disease (WNND) that resulted in between 32 and 286 fatalities each year [2]. Additionally, in 2018 Europe experienced the largest outbreak of WNV infections to date with more than 2000 cases reported [3]. Although WNV is a continuous public health threat, there is no licensed vaccine for humans.

The flavivirus genus consists of positive-sense single-stranded RNA viruses, many of which are of public health importance including yellow fever (YFV), dengue (DENV), Japanese encephalitis (JEV), and Zika (ZIKV) viruses. For the prototype flavivirus, YFV, an empirically-derived live, attenuated vaccine has been in use since the 1940s and it remains one of the most commonly administered live, attenuated vaccines decades after its development [4]. WNV belongs to the JEV serocomplex indicating that these two viruses are closely related, and although there is no licensed human vaccine for WNV, there are multiple live and inactivated vaccines for the control of JEV [5]. The most widely used is the live, attenuated vaccine strain JE SA14-14-2 [5], which was empirically derived from wild-type strain SA14, an isolate collected from a mosquito pool in 1954 [6]. The excellent safety profile of SA14-14-2 provides rationale for development of a safe and effective live, attenuated WNV vaccine.

The WNV genome is translated from a single open-reading frame that encodes ten viral proteins including the three structural proteins (capsid, membrane, and envelope) as well as the seven

Abbreviations: WNV, West Nile virus; NS5, nonstructural protein 5; MTase, methyltransferase; DENV, dengue virus; PFU, plaque-forming units; TS, temperature sensitivity; NGS, next-generation sequencing.

* Corresponding author at: Department of Pathology, University of Texas Medical Branch, Galveston, TX 77555-0436, United States.
E-mail address: abarrett@utmb.edu (A.D.T. Barrett).

https://doi.org/10.1016/j.vaccine.2019.09.045
0264-410X/

nonstructural (NS) proteins (NS1, NS2A, NS2B, NS3, NS4A, NS4B, and NS5) [7]. A safe live WNV vaccine would optimally have mutations that function by different attenuating mechanisms in multiple viral genes to prevent reversion to a virulent phenotype. Our lab has previously identified strongly attenuating mutations in the envelope, NS1, and NS4B genes [8–11], and here we report characterization of attenuating mutations in NS5.

The NS5 protein is the largest NS protein and includes an N-terminal methyltransferase (MTase) and a C-terminal RNA-dependent-RNA-polymerase (RdRp) [7]. Previous studies of WNV, JEV, YFV, and DENV have reported that the flavivirus NS5 MTase has conserved function and sequentially catalyzes N-7 methylation followed by 2′OH methylation to generate a type 1 cap on the 5′ end of the viral RNA [12–16]. Importantly, a K-D-K-E catalytic tetrad (NS5-K61-D146-K182-E218) is conserved in all flaviviruses, and therefore, data on one flavivirus should be applicable to others. The K-D-K-E tetrad (Fig. 1) catalyzes 2′O methylation, and mutation of any one of the four residues in the tetrad completely ablates 2′O methylation and strongly attenuates flaviviruses [12–16]. For example, an infectious clone based on WNV strain 3356 harboring single site substitutions of either NS5-K61A or NS5-K182A was not lethal in C3H mice inoculated subcutaneously (s.c.) with 10^5 PFU [12]. Additionally, a WNV strain 3356 clone with a NS5-E218A mutation was not lethal in C57Bl/6 mice when 10^5 PFU was inoculated by either s.c. or intracranial (i.c.) routes [13]. The strong degree of attenuation conferred by mutating the K-D-K-E tetrad provides a promising target for rational flavivirus vaccine design. One group has proposed to use MTase mutants as a tetravalent DENV vaccine candidate. Specifically, a combination of the four DENV serotypes with double mutations of K61A/E217A (or E216A depending on the DENV serotype) inoculated in AG129 mice by the i.p. route reduced viremia compared to wild-type and elicited virus-specific neutralizing antibodies and T-cell responses [16]. Additionally, DENV-2 with an E217A mutation has strongly reduced vector competence in *Aedes aegypti* mosquitoes [15].

In sum, studies in DENV as well as WNV support the use of NS5 MTase mutants in vaccine design. To further characterize WNV MTase mutants in an alternative infectious clone backbone based on strain NY99 (Supplementary Table 1) using a highly susceptible outbred mouse model, we report characterization of two single site mutants at NS5-K61A and NS5-E218A, as well as double mutation of both amino acids NS5-K61A/E218A. While the single site mutants had an attenuated phenotype, surprisingly, the double mutant had a virulent phenotype.

2. Materials & methods

2.1. Cell culture

Vero African Green Monkey kidney cells and A549 human alveolar epithelial cells were grown at 37 °C with 5% CO_2 in minimum essential media (MEM) supplemented with 100 U/mL penicillin, 100 ug/mL streptomycin, 2 mM L-glutamine, 0.1 mM non-essential amino acids, and 8% fetal bovine serum.

2.2. Generation of WNV infectious clones

Viruses were generated using a WNV infectious clone based on strain NY99-flamingo 382-99 (hereafter referred to as NY99ic) [8,10,11,17,18]. Quikchange II XL Site-Directed Mutagenesis Kit (Agilent) was utilized to generate NS5-K61A and NS5-E218A single mutants, as well as an NS5-K61A/E218A double mutant. The mutagenesis primers for the K61A mutation were GACCAGCCATCTCA GTGCTGCTGTGCCCCTAGAGAC and GTCTCTAGGGGCACAGCAGCA CTGAGATGGCTGGTC, and the primers for the E218A mutation were ACTCACCCAATACATCGCGTGCGTGGAATTCCG and CGGAATT CCACGCACGCGATGTATTGGGTGAGT, listed in 5′ to 3′ direction. After mutagenesis, plasmids were transformed into MC1061 competent *E. Coli* cells and grown in 200 mL Luria broth (LB) with 100 ug/mL ampicillin. After growth for 14–16 h, bacteria were pelleted and suspended in glucose-tris-EDTA buffer. Cells were lysed using 0.2 M NaOH/1% SDS, and lysis was neutralized using 3 M KOAc. After isopropanol precipitation, the plasmid was treated with RNAse A for 60 min, then purified using phenol:chloroform:isoamyl alcohol. The purified plasmid was ethanol precipitated, then desalted and concentrated using the QiaQuick PCR purification kit (Qiagen). Preparation, purification, and *in vitro* transcription were carried out for each clone as previously described [8]. Viruses were rescued in Vero cells between 3 and 5 days post transfection, and then passaged once in Vero cells to generate the stocks utilized for the experiments described below.

2.3. Temperature sensitivity assays

Infectivity titers of virus clones were determined in duplicate with plaque assays at both 37 °C and 41 °C. Ten-fold serial dilutions of viruses (10^{-1}-10^{-6}) were added to 6-well plates of Vero cells and incubated at room temperature for 30 min. Cells were overlaid with MEM media containing 1% agar and incubated at 37 °C or 41 °C with 5% CO_2. After two days, a second overlay was

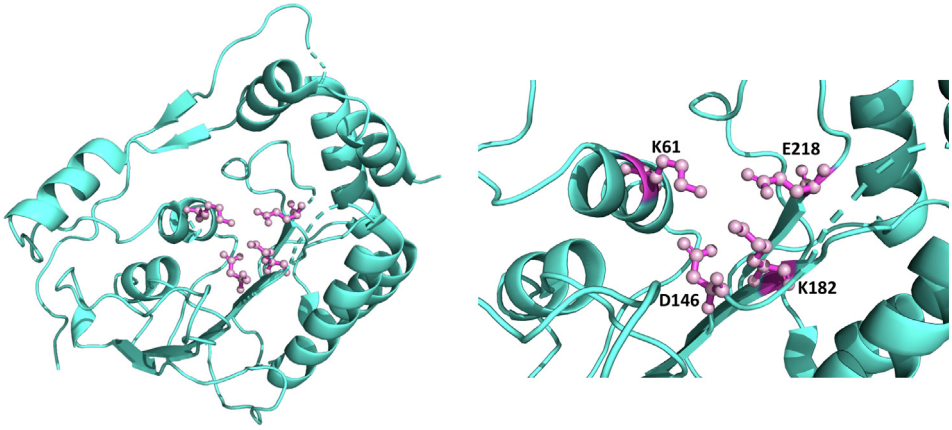

Fig. 1. Structure of WNV NS5 methyltransferase domain. Amino acids displayed in pink represent the K61-D146-K182-E218 methyltransferase catalytic tetrad.

added containing 2% neutral red dye. Plaques were counted on days three and four post-infection.

2.4. Multiplication kinetics

Duplicate flasks of Vero cells and A549 cells were infected with a multiplicity of infection (MOI) of 0.1. After incubating the virus with the cells for 30 min at room temperature, MEM containing 2% fetal bovine serum (FBS) was added to the cells and the flasks were incubated at 37 °C with 5% CO_2 for four days. At 0, 24, 36, 48, 72, and 96 h post-infection (hpi), two aliquots were collected from each flask, centrifuged at 2000 RPM for 5 min, and supernatants were then stored at −80 °C until titration for infectivity using plaque assays as described above.

2.5. Quantification of cytokines

A549 cells grown in 6-well plates were infected with a MOI of 0.1 with each virus. At 36 hpi, supernatants were collected from each well as described for multiplication kinetics experiments above. Samples of each supernatant were gamma irradiated to remove infectivity, and cytokines were then measured using the Bio-Plex Pro Human Cytokine 27-Plex Assay (Bio-Rad) and a Bio-Plex custom assay for human IFN-α2 and IFN-β. Bio-Plex assays were performed according to the manufacturer's guidelines. Cytokine levels were compared between NY99ic and each mutant by using a Kruskal-Wallis test with Dunn's multiple comparisons.

2.6. Mouse infection

Groups of five 4 week-old female Swiss Webster outbred mice (Taconic Farms, Germantown, NY) were utilized to evaluate attenuation of neuroinvasion. Each virus was inoculated by the intraperitoneal (i.p.) route with an inoculum of 500 PFU, and mice that survived through 35 days post-infection (dpi) were challenged with a 10,000 PFU i.p. dose of NY99ic (≥1000 LD_{50}). Additional groups of mice were also inoculated using an undiluted inoculum of each mutant and monitored for 28 dpi for survival. All animal experiments complied with the National Institutes of Health guide for the care and use of laboratory animals.

2.7. Isolation of virus from mouse brain

Brains were harvested from four mice that succumbed to a 500 PFU inoculum of the NS5-K61A/E218A double mutant. The brains were frozen at −80 °C until homogenization. Approximately half of each brain was homogenized with 30 cycles/second for two minutes in 500 uL of MEM with 2% FBS using the Qiagen TissueLyser II. Homogenates were immediately placed on ice prior to centrifugation at 4 °C at a speed of 10,000 RPM for 10 min. The supernatants were collected and immediately titrated using plaque assays prior to storage at −80 °C.

2.8. Sequencing analysis

RNA was extracted from Vero cell culture supernatant or from mouse brain homogenate using the QiaAmp Viral RNA Kit (Qiagen). RNA from mouse brain homogenate was amplified using PCR primers specific to the NS5 protein, and PCR products were then purified using the QiaQuick PCR Purification Kit (Qiagen) prior to Sanger sequencing. For next-generation sequencing of cell culture derived viral RNA, paired-end reads were sequenced on the Illumina NextSeq 550 platform. Trimmomatic was utilized to remove adapters and any sequences with a quality score below 30. The trimmed reads were aligned to a NY99ic reference sequence using Bowtie2 with the very sensitive local parameter. All reads were sorted based on genome position and coordinate position using SAMtools, and PCR duplicates were marked and removed using Picard Tools (Broad Institute) with the optical duplicate pixel distance set to 0. Depth of coverage was measured with SAMtools. LoFreq was utilized to measure single nucleotide variants in the viral RNA populations, and variants that had a significant strand bias ($p < 0.001$ with chi-square test or Fishers exact test) were not included in the analysis [19]. Individual sequencing contigs were visualized in Tablet software (James Hutton Institute) [20].

2.9. Molecular rendering

Pymol was utilized to model the NS5 methyltransferase of WNV (PDB 2OY0) and DENV-2 (PDB 2P3Q).

3. Results

3.1. Recovery of NS5 mutants

Single site mutants NS5-K61A and NS5-E218A and the double mutant NS5-K61A/E218A were recovered with no compensatory mutations identified in the genomic consensus sequences, and each had a similar infectivity titer to NY99ic (Table 1). Infectivity titers were measured at both 37 °C and 41 °C to determine if any of the mutants had a temperature sensitive (TS) phenotype. NY99ic had a similar infectivity titer at both 37 °C and 41 °C. Similarly, NS5-K61A and NS5-E218A mutations did not cause a significant reduction in infectivity titer at 41 °C, whereas, the double mutant NS5-K61A/E218A had a significant reduction of 1.1 $\log_{10}$ PFU at 41 °C compared to 37 °C, demonstrating that the combination of the two mutations together induced a TS phenotype (Table 1).

3.2. Multiplication kinetics in Vero and A549 cells

Multiplication kinetics of the three mutants were measured compared to the NY99ic parent in both Vero (IFN-I deficient) and A549 (IFN-I competent) cell lines. In Vero cells, all three mutants had reduced multiplication kinetics compared to NY99ic from 24 to 96 hpi, with the most significant differences occurring between 24 and 36 hpi (Fig. 2a). The NS5-K61A and NS5-E218A mutants had the largest decrease in multiplication kinetics at 24 hpi, at which time each had >100-fold reduction in titer compared to NY99ic (Fig. 2a). At 24 hpi, the NS5-K61A/E218A double mutant had a phenotype more closely resembling wild-type than the NS5 single mutants, but at 36 hpi, all three NS5 mutants had >10-fold reduction in titer compared to NY99ic (Fig. 2a).

In A549 cells, the mutants most closely resembled NY99ic at 24 hpi, however, each mutant had notably reduced infectivity titers compared to the parent strain between 36 and 96 hpi (Fig. 2b). After reaching peak titers by 36 hpi, the infectivity kinetics for each virus remained relatively constant throughout the remainder of the time points measured. While both NS5-E218A and NS5-K61A/E218A had approximately 10-fold lower infectivity titers

Table 1
Temperature sensitive phenotype in Vero cells.

	37°	41°	Delta
	$\log_{10}$ PFU/mL		
NY99ic	8.2	8.1	0.1
K61A	7.3	7.1	0.2
E218A	7.3	6.9	0.4
K61A/E218A	8.5	7.4	1.1

PFU/mL = plaque = forming units per mililiter.

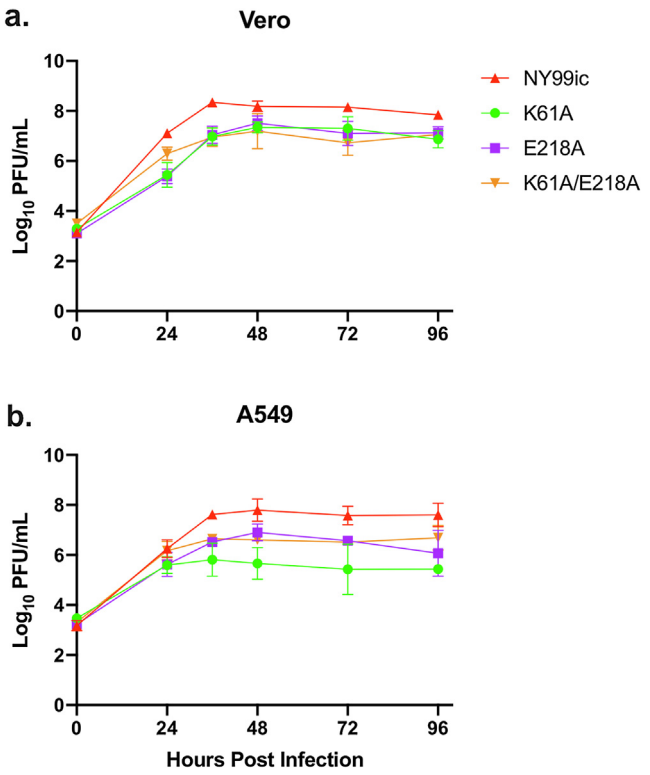

Fig. 2. Multiplication kinetics in Vero and A549 cells at a moi of 0.1 measured at 37 °C.

than NY99ic between 36 and 96 hpi, the NS5-K61A mutant had a 100-fold reduction in titer compared to NY99ic (Fig. 2b).

In both Vero and A549 cell lines, the NS5-K61A and NS5-E218A mutants each exhibited milder cytopathic effect (CPE) compared to NY99ic and the NS5-K61A/E218A double mutant. In addition, CPE in cells infected with the NS5 single mutants was not visible until approximately 72 hpi, whereas NY99ic and NS5 double mutant infected cells had apparent CPE by 48 hpi.

3.3. Induction of cytokines and chemokines in A549 cells

Cytokine and chemokine production was measured in the cell culture supernatant of human A549 cells at 36 hpi as this was the time point with maximum infectivity production but there was minimal cytopathic effect evident. Seven cytokines (IL-1β, IL-12 p70, IL-1ra, IL-10, IL-15, IL-17, PDGF) were not detected in any of the five replicate samples tested or were only measured in very low quantities of <1 pg/mL in less than half of the replicates tested, which may be a limitation of A549 cells or of the specific time point analyzed. Sixteen cytokines and chemokines had no statistical difference in the quantities induced when comparing each of the mutants to NY99ic, while six (IL-6, TNF-α, G-CSF, CXCL10, CCL2, and CCL5) had differential induction amongst the viruses tested (Supplementary Table 2). The pro-inflammatory cytokines IL-6 and TNF-α had decreased production from NS5-E218A infected cells compared to NY99ic, however, neither NS5-K61A nor NS5-K61A/E218A mutation modified the IL-6 or TNF-α pro-inflammatory response compared to NY99ic (Fig. 3). The double mutant induced a significant increase in G-CSF, whereas neither of the single mutants caused any change from NY99ic (Fig. 3). Each mutant caused an increase in chemokine expression compared to NY99ic-infected cells, including higher levels of CXCL10, CCL2, and/or CCL5 (Fig. 3). In sum, all three NS5 mutants altered inflammatory cytokine or chemokine production, however, each mutant had a unique cytokine/chemokine profile.

3.4. Mouse attenuated phenotype

Studies in highly susceptible NIH Swiss Webster outbred mice were undertaken to investigate the mouse neuroinvasive phenotype following i.p. inoculation of virus. NY99ic was strongly neuroinvasive and caused lethality in all mice between 8 and 12 days post infection (dpi) with an inoculum of 500 PFU, whereas, both NS5-K61A and NS5-E218A mutations were strongly attenuated for neuroinvasiveness, as all mice survived a relatively low inoculum of 500 PFU as well as a high inoculum of 290,000 PFU and 380,000 PFU, respectively (Table 2). Furthermore, no mice infected with NS5-K61A or NS5-E218A exhibited clinical signs of neurological disease. Although both single mutants were attenuated, the NS5-K61A/E218A double mutant was less attenuated. Three of ten mice survived from the 500 PFU inoculum of NS5-K61A/E218A, and three of five mice survived from a very high inoculum of >40,000,000 PFU (Table 2). Mice that survived 500 PFU of each mutant were also protected from a lethal NY99ic challenge, demonstrating induction of a protective immune response (Table 2). The mice that succumbed to infection with the double mutant exhibited symptoms including paralysis, slow movement, and dehydration. Overall, the double mutant did demonstrate mild attenuation of neuroinvasion and longer average survival time compared to NY99ic, however, it was less attenuated than each of the single mutants and the virulence of the double mutant was not dose-dependent.

3.5. Virus isolation from mouse brain

Virus was harvested from the brains of four mice that succumbed to the 500 PFU inoculum of the NS5-K61A/E218A mutant. Three of the mouse brains had viral infectivity titers >4 $\log_{10}$ PFU/g, while one of the brains had an infectivity titer >8 $\log_{10}$ PFU/g (Table 3). Sanger sequencing of the NS5 MTase domain verified that each virus reverted to the wild-type amino acid residues NS5-A61K/A218E (Table 3).

3.6. Next-Generation sequencing of viruses

To further investigate the instability of the genotype of the NS5-K61A/E218A mutant, next-generation sequencing (NGS) analysis was undertaken on the Vero cell P0, P1, and P5 virus stocks. It is well established that RNA viruses exist in diverse mutant swarms, or quasispecies, due to the error-prone RNA-dependent-RNA-polymerase [21], therefore, the NGS data were utilized to measure diversity in each of the viral populations. Since the P1 virus stocks were used in the mouse studies, these viruses were the focus of the quasispecies analysis. Average sequencing coverage for the P1 viruses was found to be similar and ranged between 7589–7796 for NY99ic and the NS5-K61A, NS5-E218A, and NS5-K61A/E218A mutants. Therefore, each sequencing file was analyzed for single nucleotide variants (SNVs) without downsampling. As expected for RNA viruses, many SNV subpopulations were detected in each virus (Fig. 4). In order to narrow the analysis to SNVs that were most prominent only SNVs that comprised 1% or greater of the total RNA population were investigated. NY99ic had eleven SNVs detected above 1%, whereas, the NS5-K61A mutant had 34, the NS5-E218A mutant had 21, and the NS5 double mutant had nine. Although the NS5-K61A/E218A double mutant had only nine significant SNVs, three of these encoded reversions of A61K and A218E (Table 4). Specifically, SNVs at nucleotides 7861 and 7862 were encoded simultaneously (observed on Tablet software), and taken together these two nucleotide changes cause reversion from

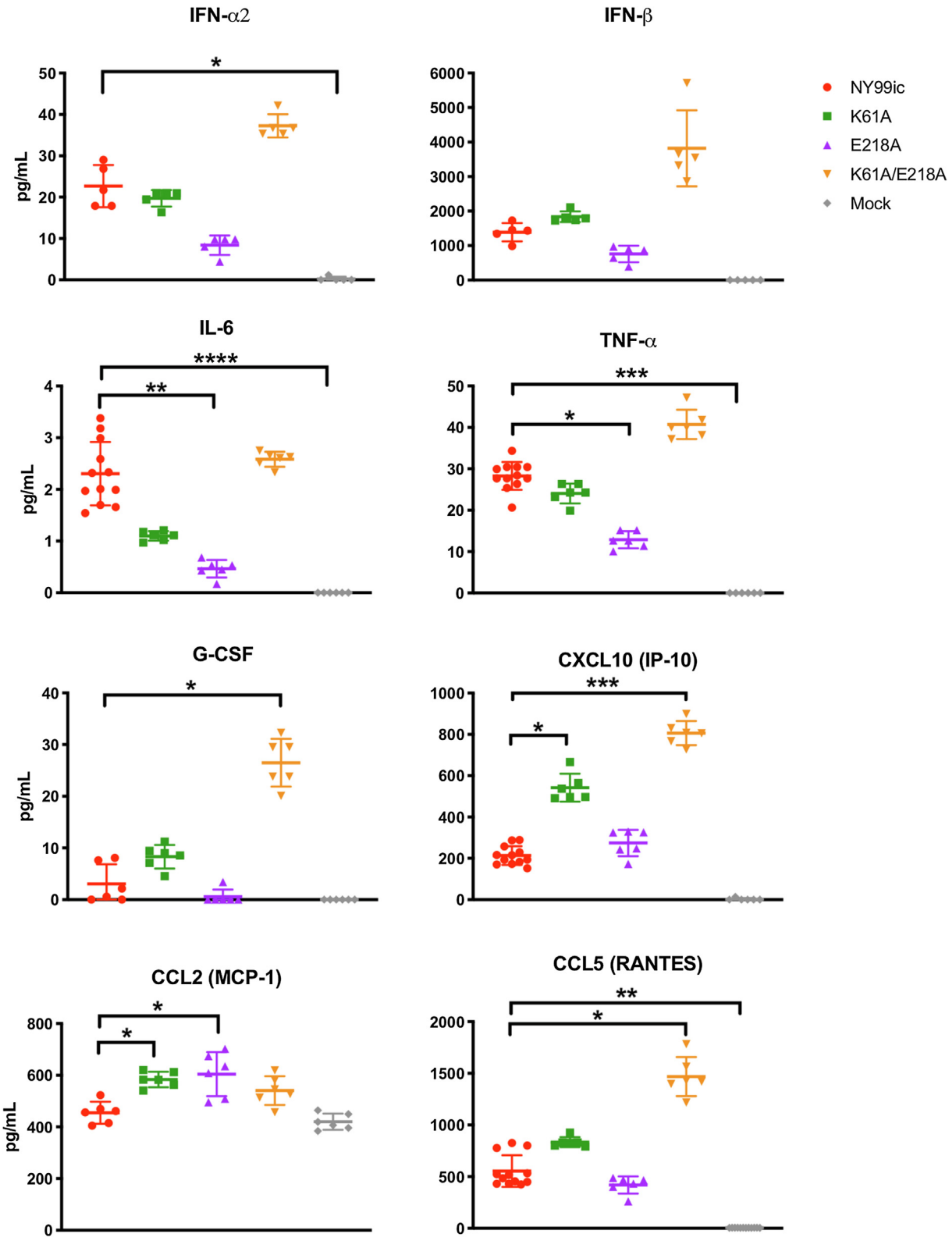

Fig. 3. Extracellular cytokines Measured at 36 hpi in A549 cell supernatants. * $p < 0.05$, ** $p < 0.01$, *** $p < 0.001$ **** $p < 0.0001$ in Kruskal-Wallis test with Dunn's multiple comparisons. IFN = interferon, IL = interleukin, TNF = tumor necrosis factor, G-CSF = granulocyte colony-stimulating factor, CXCL and CCL = chemokine ligand, IP = interferon gamma-induced protein, MCP = monocyte chemoattractant protein, RANTES = regulated on activation, normal T cell expressed and secreted.

alanine to lysine at amino acid 61. The SNV observed at nucleotide 8333 encodes reversion from alanine to glutamic acid at amino acid 218. There was no evidence of any modification to the two catalytic tetrad residues that were not mutated, NS5-D146 and NS5-K182. Upon rescue of the double mutant, the P0 stock of the virus had A61K and A218E reversions in 3.3% and 2.8% of the viral RNA population, respectively (Table 5). After a single passage (P1) in Vero cells, the A61K reversion had increased to 5.0% of the viral

Table 2
Survival analysis.

Virus	# Mice survived 500 PFU	Average Survival Time (days) ± SD	# Mice protected 10^4 PFU NY99ic challenge	Dose (PFU)	Survival
NY99ic	0/10	9.4 ± 1.3	n.d.	n.d.	n.d.
K61A	5/5	>35	5/5	2.9×10^5	5/5
E218A	5/5	>35	5/5	3.8×10^5	5/5
K61A/E218A	3/10	#*11.1 ± 1.7	2/2	4.2×10^7	3/5

Groups of five 5–6 week-old NIH Swiss Webster outbred mice were inoculated by the intraperitoneal (i.p.) route.
PFU = plaque-forming units.
SD = standard deviation.
Significance was tested using a Mann Whitney test to compare mutant survival time to NY99ic survival time.
Calculated from mice that died.
* p = 0.02.

Table 3
Mouse brain-derived virus titers and consensus sequences.

	Time of death (days post infection)	Viral titer in brain (log_{10} PFU/gram)	Consensus sequence at nucleotide 7861 (NS5-61) [amino acid]	Consensus sequence at nucleotide 8333 (NS5-218) [amino acid]
Input Virus	–	–	GCA [A]	GCG [A]
Mouse 1	8	8.7	AAA [K]	GAG [E]
Mouse 2	10	4.9	AAA [K]	GAG [E]
Mouse 3	12	4.9	AAA [K]	GAG [E]
Mouse 4	12	4.4	AAA [K]	GAG [E]

Brains were harvested from mice that died from the 500 PFU intraperitoneal inoculation of the NS5-K61A/E218A mutant.
PFU = plaque-forming units.

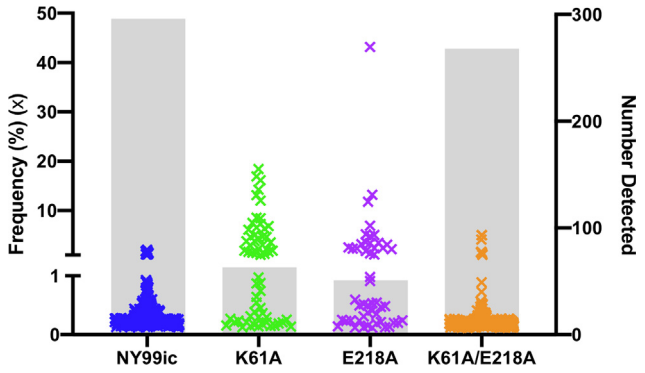

Fig. 4. Single nucleotide variant profiles of P1 virus stocks. Each 'x' represents the frequency of a SNV, and the grey bars display the total number of SNVs detected.

RNA population, while the A218E reversion had increased to 4.1% (Tables 4 and 5). After five passages in Vero cells (P5), the NS5-K61A/E218A double mutant did not revert to a wild-type consensus sequence, but 41% of the viral RNA population encoded reversion at residue NS5-61 and 47.6% encoded reversion at residue NS5-218, suggesting that further passage may yield reversion in the consensus sequence (Table 5). In comparison, both NS5-K61A and NS5-E218A single mutants had no SNVs of >1% frequency that encoded reversion in P0, P1, or P5 stocks (Tables 4 and 5). Although SNVs as low as 0.1% could be detected, the P5 NS5-K61A mutant had no evidence of reversion even at very low levels. Alternatively, the P5 NS5-E218A mutant had a SNV encoding A218E reversion in 0.2% of the viral RNA population. Shannon entropy was also calculated on P1 stocks of each virus as an alternative measurement of diversity for each mutant as has been described in previous reports [22,23], and the results reflected the patterns displayed in the SNVs in Table 4 in which NY99ic and the NS5-K61A/E218A mutant have low levels of entropy across the genome, and the NS5-K61A and NS5-E218A mutants have higher peaks of entropy across the genome (data not shown).

4. Discussion

WNV NS5-K61A and NS5-E218A mutants have previously been characterized in an infectious clone based on WNV strain 3356 isolated from New York in 2000 [12,13]. The mutants generated for this study utilized a different WNV strain backbone based off of a similar strain of WNV from New York in 1999 (NY99ic), however, there are 27 nucleotide differences and seven amino acid substitutions between the two clones, including a valine to alanine substitution in the MTase domain of NS5 (Supplementary Table 1) [8,24]. Additionally, double mutation in the NS5 MTase catalytic tetrad has previously been proposed as a vaccine candidate for the four DENV serotypes, however, the homologous mutations had not been investigated in WNV prior to this study. Therefore, this paper describes the characterization of NS5-K61A and NS5-E218A mutations in an alternative model to that which was used by other groups, while simultaneously reporting the first investigation of combined NS5-K61A/E218A mutations in WNV.

Consistent with published data using inbred mice, NS5-K61A or NS5-E218A mutation caused no lethality in outbred mice when inoculated peripherally with ≥100,000 PFU (Table 2). Significantly, relatively low 500 PFU doses of NS5-K61A and NS5-E218A mutants both induced productive immune responses capable of protecting mice from lethal WNV challenge (Table 2). As our previous work with attenuated WNV NS1 and NS4B mutants found a correlation between low viremia and attenuated neuroinvasion [9–11], it is possible that the NS5 MTase mutants do not replicate to high viremia and thus cannot invade the central nervous system. This speculation is in agreement with the observation that the MTase mutants are sensitive to the antiviral effects of IFIT proteins [13].

Previous studies reported that double mutation of NS5-K61A/E217A (or E216A) in the KDKE tetrad was attenuating for the four DENV serotypes [16], but surprisingly, in WNV the double mutation caused a reduction of attenuation compared to mutation of either NS5-K61A or NS5-E218A alone. It was hypothesized that the double mutant had reduced attenuation *in vivo* due to the instability of the combined MTase mutations, and this was confirmed by Sanger sequencing of mouse-brain derived viruses.

Table 4
Summary of single nucleotide variants > 1% of viral RNA populations in P1 cell culture stocks of NY99ic and each NS5 mutant.

	Nucleotide Position	Major Nucleotide	Minor Nucleotide	Viral Protein Position	Major Residue	Minor Residue	Frequency (%)
NY99ic	103	A	G	C-3	K	E	2.1
	106	A	G	C-4	K	E	2.0
	532	A	U	prM-23	I	F	1.7
	653	A	C	prM-63	E	A	1.1
	981	A	G	E-5	G	G	1.9
	1072	A	G	E-36	K	E	1.7
	1588	A	U	E-208	T	S	1.5
	2135	A	G	E-390	E	G	1.4
	5952	A	U	NS3-447	P	P	1.0
	7981	A	C	NS5-101	R	R	1.4
	9278	A	U	NS5-533	Y	F	1.2
K61A	106	A	C	C-4	K	Q	6.6
	306	A	G	C-70	R	R	4.6
	307	G	A	C-71	G	S	4.7
	388	C	A	C-98	R	R	8.6
	489	G	A	prM-8	G	G	6.9
	492	G	A	prM-9	K	K	3.6
	507	A	G	prM-14	V	V	16.1
	756	G	A	prM-97	Q	Q	14.2
	768	A	G	prM-101	E	E	1.5
	788	A	G	prM-108	K	R	13.1
	1415	A	G	E-150	E	G	2.2
	2184	A	G	E-406	K	K	6.3
	2798	A	G	NS1-110	K	R	5.0
	3337	A	G	NS1-290	S	G	2.9
	4387	A	G	NS2B-57	T	A	1.9
	4540	A	G	NS2B-108	S	G	7.5
	4740	A	G	NS3-43	E	E	1.9
	4862	A	G	NS3-84	K	R	2.2
	5925	A	G	NS3-438	G	G	1.6
	6106	A	C	NS3-499	I	L	6.1
	6197	A	G	NS3-529	E	G	3.0
	6295	A	G	NS3-562	R	G	1.0
	7015	U	C	NS4B-34	L	L	16.9
	7578	A	G	NS4B-221	T	T	1.4
	8815	A	G	NS5-379	T	A	18.5
	8947	A	U	NS5-423	S	C	4.4
	9092	A	G	NS5-471	K	R	3.8
	9570	A	G	NS5-630	G	G	3.8
	9766	A	G	NS5-696	I	V	7.3
	9936	C	A	NS5-752	N	K	4.7
	10,417	A	G	3′ UTR	–	–	8.4
	10,807	A	G	3′ UTR	–	–	12.0
	10,814	A	U	3′ UTR	–	–	1.6
	10,888	U	A	3′ UTR	–	–	1.2
E218A	353	A	G	C-86	K	R	2.5
	555	A	G	prM-30	G	G	2.4
	557	A	G	prM-31	K	R	2.4
	1303	A	G	E-113	I	V	3.1
	1525	A	G	E-187	T	A	5.2
	1531	G	A	E-189	D	N	3.5
	1996	G	A	E-344	A	T	13.2
	2148	U	C	E-394	N	N	2.3
	2176	A	G	E-404	I	V	3.2
	4479	C	G	NS2B-87	L	L	3.4
	4686	C	U	NS3-25	I	I	3.6
	4976	A	G	NS3-122	E	G	11.8
	5684	A	G	NS3-358	K	R	6.9
	5713	A	G	NS3-368	M	V	2.1
	7427	A	G	NS4B-171	K	R	2.3
	7557	A	G	NS4B-214	A	A	4.8
	7768	G	A	NS5-30	E	K	5.0
	9160	C	U	NS5-494	L	F	1.3
	9855	U	C	NS5-725	D	D	1.1
	9863	C	U	NS5-728	T	I	43.1
	10,814	A	U	3′ UTR	–	–	1.8

(*continued on next page*)

Table 4 (*continued*)

	Nucleotide Position	Major Nucleotide	Minor Nucleotide	Viral Protein Position	Major Residue	Minor Residue	Frequency (%)
K61A/E218A	285	A	G	C-63	R	R	1.6
	763	G	C	prM-100	G	R	1.4
	5166	G	A	NS3-185	R	R	1.0
	6686	A	C	NS4A-73	Q	P	1.6
	7657	A	U	NS4B-248	M	L	1.6
	7861	G	A	NS5-61	*A	*K	5.0
	7862	C	A	NS5-61			
	8333	C	A	NS5-218	A	E	4.1
	10,814	A	U	3′ UTR	–	–	1.2

* SNVs at nucleotide 7861 and 7862 were encoded simultaneously.

Table 5
Evidence of reversion of the NS5-K61A/E218A mutant increases after Vero cell passage.

Virus	P0	P1	P5
K61A	<0.1%	<0.1%	<0.1%
E218A	<0.1%	<0.1%	0.2%
K61A/E218A	3.3%/2.8%	5.0%/4.1%	41%/47%

The frequency of reversion in single nucleotide variants (SNVs) of cell culture stocks of each NS5 mutant are listed. The limit of SNV detection for the LoFreq analysis was 0.1%.
P0, P1, P5 = Vero cell passage 0, 1, or 5.

NGS analysis of the Vero cell P1 NS5-K61A/E218A mutant that was used to inoculate mice revealed SNV subpopulations that encoded reversions of both mutations. Importantly, the reversion of NS5-A61K required the first two nucleotides in the codon to change (AAA to GCA), indicating the strong selective pressure on the virus to restore the wild-type genotype and MTase activity. To make the NS5-E218A mutation, only one nucleotide in the codon could be changed (GAG to GCG) due to the codon similarity; therefore, the A218E reversion only required a single nucleotide substitution. Although the P1 stocks of the single mutants that were used in the mouse studies had more SNVs >1% detected across the genome, none encoded reversion. NS5-K61A had no SNVs in the MTase domain at all (NS5 amino acids 1-267), while NS5-E218A only had one SNV in the MTase at amino acid 30, which is not structurally neighboring the MTase catalytic tetrad. While the double mutant had few SNVs detected overall, three out of nine encoded reversion. Although the NGS reads were not long enough to show whether or not the A61K and A218E reversions were encoded on the same sequencing contigs, we hypothesize that the reversions occurred simultaneously since the virus would be expected to have an attenuated phenotype if either of the mutations remained. Interestingly, for all four DENV serotypes, double mutation of NS5-K61A/E217A (or E216A) was stable in the consensus sequences after five passages in Vero cells [16,25], and the consensus genome of the double mutant was also stable in our study after five passages of the WNV mutant in Vero cells; however, there was >40% reversion to wild-type evident in the SNVs indicating the consensus sequence may revert upon continued passage. The P5 stock of the NS5-K61A mutant had no evidence of reversion, but the P5 stock of NS5-E218A had a small 0.2% SNV encoding reversion. The small A218E SNV in the P5 NS5-E218A mutant could potentially decrease the attenuation of this mutant, but it is unclear how high SNV frequency has to be to impact pathogenicity.

Along with investigation of reversion in SNVs, a NS5-T728I variant stood out for its high frequency (43.1%) in the P1 virus stock of the attenuated NS5-E218A mutant (Table 4). Residue NS5-728 resides in the thumb region of the RdRp, and this region is important for providing ssRNA access to the catalytic site in the palm domain [26]. NS5-728 resides in the interface between the thumb and palm domain [26], so it is possible that the SNV at this residue alters ssRNA access to the RdRp catalytic site. This could potentially attribute to the increased multiplication kinetics of the NS5-E218A mutant compared to the NS5-K61A mutant, but additional studies are needed to better understand how the NS5-T728I mutation may influence the WNV phenotype. Of note, the P5 virus stock of the NS5-E218A mutant retained this SNV in 41% of viral RNA, so the frequency remained fairly constant following five cell culture passages.

Despite conserved amino acids and functions of the KDKE catalytic tetrads, differences in the DENV and WNV MTase could allow double mutation in the MTase catalytic tetrad to be stable in DENV but not in WNV. Structural studies have identified the GTP-binding domain required for MTase function in DENV, and one of the key amino acids, proline at NS5-152, is a serine in WNV (Fig. 5) [27]. It is possible that DENV and WNV have a different affinity for GTP-binding that permits stability of double mutations in the DENV MTase, but not in WNV [27], however, GTP-binding affinities of WNV and DENV NS5 proteins have not been compared.

The MTase single mutants were similar to those previously studied in that the largest reductions in multiplication kinetics in Vero cells compared to wild-type were between 24 and 36 hpi, but in contrast to other studies [12], the NS5-K61A and NS5-E218A mutants had similar kinetics to one another (Fig. 2a). In DENV-2, NS5-K61A/E217A mutations caused approximately 10-fold reduction in Vero cell multiplication kinetics from 24 to 120 hpi compared to wild-type, and the DENV-2 double mutant had lower infectivity titers at 48 hpi compared to either of the single mutants [15]. In WNV, double mutation in the MTase domain did

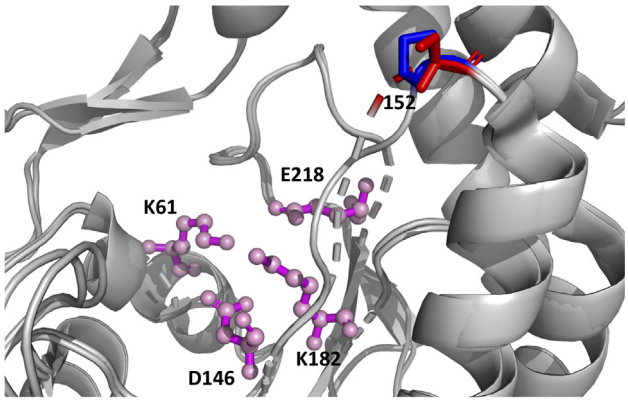

Fig. 5. Structural alignment of WNV and DENV NS5 methyltransferase. The catalytic tetrad is shown in magenta. Proline152 in DENV is shown in blue, while Serine152 in WNV is shown in red.

not decrease multiplication kinetics compared to either of the single mutants, and at 24 hpi the double mutant had an infectivity titer that was higher than either of the single mutants and was approaching that of NY99ic (Fig. 2a). Therefore, Vero cell multiplication kinetics indicated that the NS5-K61A/E218A had a different phenotype than that which was observed for DENV-2 and for the WNV MTase single mutants. However, this different phenotype may be contributed by the 4–5% wild-type reversion of the double mutant P1 seed that outcompetes the double mutant virus replication during multiplication at a MOI of 0.1.

In previous studies, WNV and DENV MTase mutants were found to have increased sensitivity to the antiviral activity of IFN-I induced IFIT proteins compared to wild-type WNV, but they induced equivalent levels of IFN- β [13,15]. Although IFN-α and IFN-β levels were not statistically different when comparing the WNV NS5 mutants to NY99ic, it is notable that the NS5-K61A/E218A mutant exhibited a trend toward increased IFN-I production (Fig. 3). The NS5-K61A mutant had the greatest reduction in A549 cell multiplication kinetics (Fig. 2b), indicating that this mutant may be more sensitive to IFN-I signaling than NS5-E218A or NS5-K61A/E218A. Despite differences in viral titer, both single mutants increased levels of CCL2 compared to NY99ic, but only NS5-E218A caused a decrease in pro-inflammatory cytokines IL-6 and TNF-α, and only NS5-K61A increased the induction of CXCL10. Either of the observed innate immune modifications could be protective, considering high levels of inflammatory cytokines could increase WNV neuroinvasion [28,29], and both CCL2 and CXCL10 are important chemokines for protection from WNV neurological disease [30–33]. The NS5-K61A/E218A double mutant induced significantly more G-CSF, CXCL10, and CCL5 compared to NY99ic. While G-CSF is not often studied in the context of WNV infection, it can function as a neuronal ligand to reduce apoptosis [34], indicating that it could contribute to protective immunity against WNV neurological disease. Likewise, both CXCL10 and CCL5 are important chemokines for WNV control in mice [30–32,35], and genetic deficiency of the CCL5 receptor, CCR5, is a risk factor for symptomatic WNV disease in humans [36,37]. Although the NS5-K61A/E218A mutant induced potentially protective cytokines and chemokines *in vitro*, this phenotype did not correlate with attenuation in the outbred mouse model. As described for the TS phenotypes, it is possible that the double mutant could induce a protective immune response leading to viral attenuation if the mutations were stable and could not revert to wild-type sequence.

In sum, this report describes the first genotypic and phenotypic characterization of double mutation of the NS5 MTase catalytic tetrad in WNV. Although *in vitro* studies of the NS5-K61A/E218A mutant suggested the mutations could be attenuating, the virus was more virulent than either of the MTase single mutants tested. Even though the NS5-K61A/E218A mutant did not have the attenuated phenotype expected, the independent mutations NS5-K61A and NS5-E218A were strongly attenuating and protective as was reported in previous studies using a different infectious clone and alternative animal models. Sequencing analysis of each mutant used in the mouse studies indicated that mutation of a single amino acid in WNV NS5 MTase catalytic tetrad was stable, whereas, double mutation of both amino acids simultaneously gave rise to reversion. Since the single site NS5-K61A and NS5-E218A mutations were stable and attenuated *in vivo*, they remain good candidates to consider for rational WNV vaccine development. Considering that the P5 stock of NS5-E218A had a very small frequency SNV (0.2%) encoding reversion of A218E, NS5-K61A appears to be a more stable mutation and thus may be a safer choice for inclusion in a candidate vaccine. Since a live WNV vaccine would ideally harbor multiple attenuating mutations, NS5-K61A should be characterized in the context of additional independently attenuating mutations in other viral genes.

Funding

This work was funded by a grant from Gillson Longenbaugh Foundation to ADTB. JAK was funded in part by NIH grant T32 AI 7526-16. T.W. is supported in part by NIH grant R01 AI099123 and a grant from the Sealy Institute for Vaccine Sciences at UTMB.

Author contributions

J.A.K., H.L., and T.W. performed experiments. C.Y.H. and J.A.K. designed infectious clones. S.G.W., T.G.W., and J.A.K. conducted and analyzed next-generation sequencing data. J.A.K., S.G.W., T. W., and A.D.T.B. analyzed data and prepared the manuscript.

Declaration of Competing Interest

The authors declare that they have no known competing financial interests or personal relationships that could have appeared to influence the work reported in this paper.

Appendix A. Supplementary material

Supplementary data to this article can be found online at https://doi.org/10.1016/j.vaccine.2019.09.045.

References

[1] Petersen LR, Brault AC, Nasci RS. West Nile virus: review of the literature. JAMA 2013;310:308–15.
[2] West Nile Virus- Statistics and Maps. Centers for Disease Control and Prevention. https://www.cdc.gov/westnile/statsmaps/index.html [2019, accessed 5 July 2019].
[3] Barrett A. West Nile in Europe: An increasing public health problem. J Travel Med;25.
[4] Beck AS, Barrett ADT. Current status and future prospects of yellow fever vaccines. Expert Rev Vacc 2015;14:1479–92.
[5] International Travel and Health- Vaccines. World Health Organization. http://www.who.int/ith/vaccines/japanese_encephalitis/en/ [2018, accessed 3 October 2018].
[6] Ni H, Burns NJ, Chang G-JJ, Zhang M-J, Wills MR, et al. Comparison of nucleotide and deduced amino acid sequence of the 5′ non-coding region and structural protein genes of the wild-type Japanese encephalitis virus strain SA14 and its attenuated vaccine derivatives. J Gen Virol 1994;75:1505–10.
[7] Klema VJ, Padmanabhan R, Choi KH. Flaviviral Replication Complex: Coordination between RNA Synthesis and 5′-RNA Capping. 2015;4640–56.
[8] Beasley DWC, Whiteman MC, Zhang S, Huang CY, Schneider BS, et al. Envelope protein glycosylation status influences mouse neuroinvasion phenotype of genetic lineage 1 west nile virus strains envelope protein glycosylation status influences mouse neuroinvasion phenotype of genetic lineage 1 west nile virus strains. J Virol 2005;79:8339–47.
[9] Whiteman MC, Wicker JA, Kinney RM, Huang CYH, Solomon T, et al. Multiple amino acid changes at the first glycosylation motif in NS1 protein of West Nile virus are necessary for complete attenuation for mouse neuroinvasiveness. Vaccine 2011;29:9702–10.
[10] Wicker JA, Whiteman MC, Beasley DWC, Davis CT, Zhang S, et al. A single amino acid substitution in the central portion of the West Nile virus NS4B protein confers a highly attenuated phenotype in mice. Virology 2006;349:245–53.
[11] Wicker JA, Whiteman MC, Beasley DWC, Davis CT, McGee CE, et al. Mutational analysis of the West Nile virus NS4B protein. Virology 2012;426:22–33.
[12] Zhou Y, Ray D, Zhao Y, Dong H, Ren S, et al. Structure and function of flavivirus NS5 methyltransferase. J Virol 2007;81:3891–903.
[13] Daffis S, Szretter KJ, Schriewer J, Li J, Youn S, et al. 2′-O methylation of the viral mRNA cap evades host restriction by IFIT family members. Nature 2011;468:452–6.
[14] Li S-H, Dong H, Li X-F, Xie X, Zhao H, et al. Rational design of a flavivirus vaccine by abolishing viral RNA 2′-O methylation. J Virol 2013;87:5812–9.
[15] Zust R, Dong H, Li X, Chang DC, Zhang B, et al. Rational Design of a Live Attenuated Dengue Vaccine : 2′-O-Methyltransferase Mutants Are Highly Attenuated and Immunogenic in Mice and Macaques. Plos Pathog 2013;9. https://doi.org/10.1371/journal.ppat.1003521.
[16] Züst R, Li SH, Xie X, Velumani S, Chng M, et al. Characterization of a candidate tetravalent vaccine based on 2′-O-methyltransferase mutants. PLoS ONE 2017;13:1–19.
[17] Zhang S, Li L, Woodson SE, Huang CY, Kinney RM, et al. A mutation in the envelope protein fusion loop attenuates mouse neuroinvasiveness of the NY99 strain of West Nile virus. Virology 2006;353:35–40.

[18] Whiteman MC, Li L, Wicker JA, Kinney RM, Huang C, et al. Development and characterization of non-glycosylated E and NS1 mutant viruses as a potential candidate vaccine for West Nile virus. Vaccine 2010;28:1075–83.
[19] Wilm A, Aw PPK, Bertrand D, Yeo GHT, Ong SH, et al. LoFreq: A sequence-quality aware, ultra-sensitive variant caller for uncovering cell-population heterogeneity from high-throughput sequencing datasets. Nucl Acids Res 2012;40:11189–201.
[20] Milne I, Stephen G, Bayer M, Cock PJA, Pritchard L, et al. Using Tablet for visual exploration of second-generation sequencing data. Brief Bioinform 2012;14:193–202.
[21] Grubaugh ND, Fauver JR, Rückert C, Weger-Lucarelli J, Garcia-Luna S, et al. Mosquitoes transmit unique west nile virus populations during each feeding episode. Cell Rep 2017;19:709–18.
[22] Beck A, Tesh RB, Wood TG, Widen SG, Ryman KD, et al. Comparison of the live attenuated yellow fever vaccine 17D–204 strain to its virulent parental strain asibi by deep sequencing. J Infect Dis 2014;209:334–44.
[23] Collins ND, Beck AS, Widen SG, Wood TG, Higgs S, et al. Structural and nonstructural genes contribute to the genetic diversity of RNA viruses. MBio 2018;9:1–13.
[24] Shi P, Tilgner M, Lo MK, Kent KA, Bernard KA. Infectious cDNA clone of the epidemic west nile virus from New York City. J Virol 2002;76:5847–56.
[25] Fink K, Shi P-Y, Qin CF. Novel attenuated dengue virus strains for vaccine application; 2014.
[26] Malet H, Egloff M, Selisko B, Butcher RE, Wright PJ, et al. Crystal structure of the RNA polymerase domain of the west nile virus non-structural protein 5. J Biol Chem 2007;282:10678–89.
[27] Egloff MP, Benarroch D, Selisko B, Romette JL, Canard B. An RNA cap (nucleoside-2′-O-)-methyltransferase in the flavivirus RNA polymerase NS5: Crystal structure and functional characterization. EMBO J 2002;21:2757–68.
[28] Wang T, Town T, Alexopoulou L, Anderson JF, Fikrig E, et al. Toll-like receptor 3 mediates West Nile virus entry into the brain causing lethal encephalitis. Nat Med 2004;10:1366–73.
[29] Kumar M, Verma S, Nerurkar VR. Pro-inflammatory cytokines derived from West Nile virus (WNV) -infected SK-N-SH cells mediate neuroinflammatory markers and neuronal death. J Neuroinflammation 2010;7:73.
[30] Qian F, Goel G, Meng H, Wang X, You F, et al. Systems Immunology Reveals Markers of Susceptibility to West Nile Virus Infection. Clin Vacc Immunol 2015;22:6–16.
[31] Zhang B, Chan YK, Lu B, Diamond MS, Klein RS, et al. CXCR3 Mediates Region-Specific Antiviral T Cell Trafficking within the Central Nervous System during West Nile Virus. J Immunol 2008;180:2641–9.
[32] Klein RS, Lin E, Zhang B, Luster AD, Tollett J, et al. Neuronal CXCL10 directs CD8 2 T-cell recruitment and control of west nile virus encephalitis. 2005;79:11457–66.
[33] Lim JK, Obara CJ, Rivollier A, Pletnev AG, Kelsall BL, et al. Chemokine receptor CCR2 is critical for monocyte accumulation and survival in west nilve virus encephalitis. J Immunol 2011;186:471–8.
[34] Schneider A, Krüger C, Steigleder T, Weber D, Pitzer C, et al. The hematopoietic factor G-CSF is a neuronal ligand that counteracts programmed cell death and drives neurogenesis. J Clin Invest 2005;115:2083–98.
[35] Glass WG, Lim JK, Cholera R, Pletnev AG, Gao J, et al. Chemokine receptor CCR5 promotes leukocyte trafficking to the brain and survival in West Nile virus infection. 202. Epub ahead of print; 2005. http://doi.org/10.1084/jem.20042530.
[36] Lim JK, Louie CY, Glaser C, Jean C, Johnson B, et al. Genetic Deficiency of Chemokine Receptor CCR5 Is a Strong Risk Factor for Symptomatic West Nile Virus Infection : A Meta-Analysis of 4 Cohorts in the US Epidemic. 197. Epub ahead of print; 2008. http://doi.org/10.1086/524691.
[37] Glass WG, Mcdermott DH, Lim JK, Lekhong S, Yu SF, et al. CCR5 deficiency increases risk of symptomatic West Nile virus infection. J Exp Med 2006;203:35–40.